Genetic Dissection of Hybrid Male Sterility Across Stages of Spermatogenesis

Denise J. Schwahn,* Richard J. Wang,† Michael A. White,†,‡ and Bret A. Payseur†,1
*Research Animal Resources Center, University of Wisconsin-Madison, Wisconsin 53726, †Laboratory of Genetics, University of Wisconsin-Madison, Wisconsin 53706, and ‡Department of Genetics, University of Georgia, Athens, Georgia 30602
ORCID ID: 0000-0002-8889-4269 (R.J.W.)

ABSTRACT Hybrid sterility is a common form of reproductive isolation between nascent species. Although hybrid sterility is routinely documented and genetically dissected in speciation studies, its developmental basis is rarely examined, especially in generations beyond the F_1 generation. To identify phenotypic and genetic determinants of hybrid male sterility from a developmental perspective, we characterized testis histology in 312 F_2 hybrids generated by intercrossing inbred strains of *Mus musculus domesticus* and *M. m. musculus*, two subspecies of house mice. Hybrids display a range of histologic abnormalities that indicate defective spermatogenesis. Among these abnormalities, we quantified decreased testis size, reductions in spermatocyte and spermatid number, increased apoptosis of meiosis I spermatocytes, and more multinucleated syncytia. Collectively, our phenotypic data point to defects in meiosis I as a primary barrier to reproduction. We identified seven quantitative trait loci (QTL) controlling five histologic traits. A region of chromosome 17 that contains *Prdm9*, a gene known to confer F_1 hybrid male sterility, affects multinucleated syncytia and round spermatids, potentially extending the phenotypic outcomes of this incompatibility. The X chromosome also plays a key role, with loci affecting multinucleated syncytia, apoptosis of round spermatids, and round spermatid numbers. We detected an epistatic interaction between QTL on chromosomes 17 and X for multinucleated syncytia. Our results refine the developmental basis of a key reproductive barrier in a classic model system for speciation genetics.

KEYWORDS speciation; hybrid sterility; testis histopathology; meiosis defect; stage VII

THE reduced fertility of hybrids constitutes a major barrier to reproduction between species (Coyne and Orr 2004). When such "hybrid sterility" has a genetic component, this barrier can become permanent and is expected to increase in severity over time. Hybrid sterility tends to evolve faster than hybrid inviability (Coyne and Orr 2004), and in species with XY sex determination, males usually evolve sterility before females (Coyne and Orr 1989), suggesting that hybrid male sterility is often the first form of postzygotic isolation to appear. The genetics of hybrid male sterility between nascent species therefore provides a window into the mechanisms of a primary determinant of speciation in the early stages of the process.

doi: https://doi.org/10.1534/genetics.118.301658
Manuscript received August 16, 2018; accepted for publication October 12, 2018; published Early Online October 17, 2018.
Supplemental material available at Figshare: https://doi.org/10.25386/genetics.7161119.
[1]Corresponding author: Laboratory of Genetics, University of Wisconsin-Madison, Genetics/Biotechnology 2428, 425-G Henry Mall, Madison, WI 53706. E-mail: bret.payseur@wisc.edu

The most direct way to evaluate hybrid male sterility is to measure the relative ability of hybrid males to sire offspring through mating experiments. Although this method focuses on the functional trait of interest, reproductive performance, it yields no insight into the phenotypic and developmental causes of sterility. A second strategy examines phenotypes known to be correlated with fertility. This approach has the potential to pinpoint the mechanisms of hybrid dysfunction, but it is rarely extended beyond assessment of a few outcomes of spermatogenesis (*e.g.*, the count, shape, and/or motility of sperm) or gross reproductive morphology (*e.g.*, testis weight). Because a variety of changes in the testis can produce similar phenotypic outcomes, measuring these traits also leaves the primary drivers of hybrid sterility unaddressed.

Ideally, the search for genetic determinants of hybrid male sterility would recognize the dynamic nature of spermatogenesis. By reproductive maturity in some species, a single testis contains mitotic stem cells (spermatogonia), two kinds of meiotic cells (primary and secondary spermatocytes),

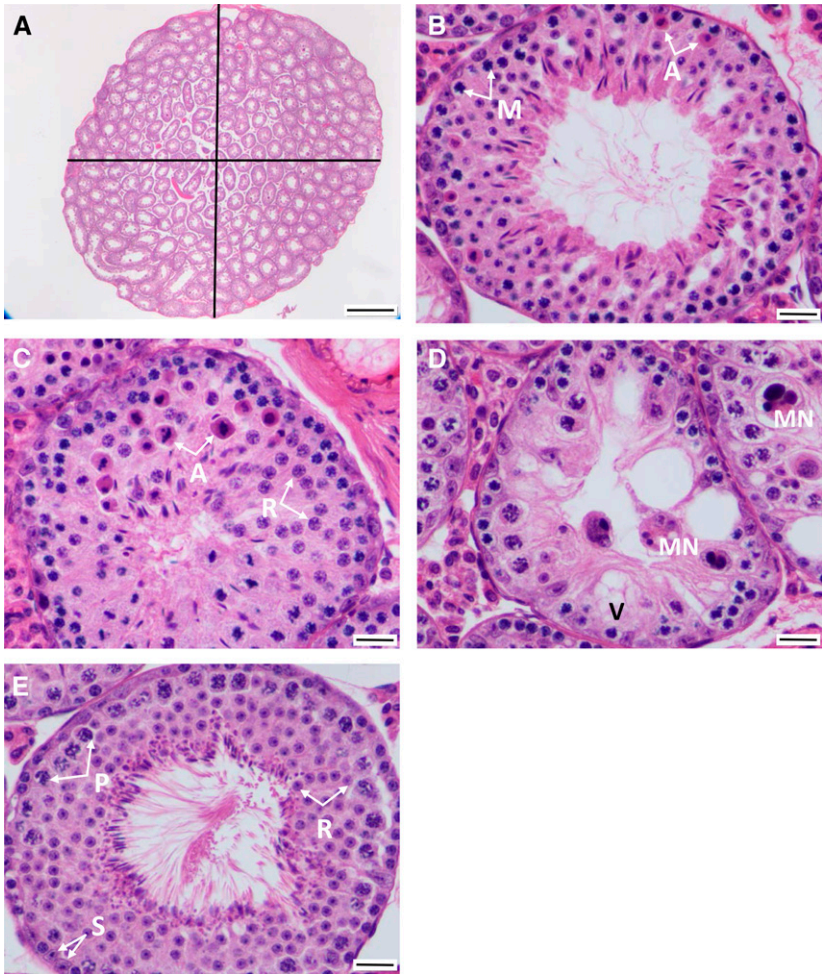

Figure 1 Schematic of testis histology measurements. (A) Entire testis. Testicular area was calculated using the area of an oval following measurements of its width and height. ×40 magnification was also used to count the number of tubules per testis. Bar, 500 μm. (B) Apoptotic meiosis I cells (A) showing hyper-eosinophilic cytoplasm and dense chromatin. Primary spermatocytes entering meiosis I (M). Bar, 20 μm. (C) Apoptosis of round spermatids (A) and round spermatocytes (R). Bar, 20 μm. (D) Multinucleated syncytia (MN; central and in adjacent tubules). Vacuolated Sertoli cell (V). Bar, 20 μm. (E) A healthy stage VII tubule used to count Sertoli cells (S), pachytene spermatocytes (P), and round spermatids (R). Bar, 20 μm.

morphologically differentiating postmeiotic cells (spermatids), and maturing sperm, as well as Sertoli ("nurse") cells and interstitial (Leydig) cells. Because spermatogenesis is continuous, these diverse cell populations can be surveyed simultaneously in individual males by histologic examination of the testis. The result is a developmental characterization of hybrid male sterility that specifies what stages of spermatogenesis are disrupted in hybrids (Oka *et al.* 2010). This increased phenotypic resolution has the potential to accelerate both the identification of the genes that determine this key reproductive barrier and the discovery of their functions.

The house mouse, *Mus musculus*, is a powerful model species for dissecting the genetics of hybrid male sterility. In the house mouse, the temporal and spatial progression of spermatogenesis in the testis is well understood, making it straightforward to identify specific histologic abnormalities in hybrids. Subspecies of house mice diverged from a common ancestor at least 350,000 years ago (Boursot *et al.* 1993; Duvaux *et al.* 2011; Geraldes *et al.* 2011) and display partial reproductive isolation (Forejt and Ivanyi 1974; Alibert *et al.* 1997; Britton-Davidian *et al.* 2005; Good *et al.* 2008b; Turner *et al.* 2012; White *et al.* 2012). Therefore, house mice provide insights into hybrid male sterility as it evolves (Wang *et al.* 2015).

Reproductive isolation between two subspecies of mice, *Mus musculus domesticus* (the Western European house mouse) and *M. m. musculus* (the Eastern European house mouse), has been intensively studied. These subspecies meet and mate in a natural hybrid zone that stretches across Europe. Allele frequency clines are narrow relative to subspecies ranges, suggesting that reproductive isolation limits gene flow (Tucker *et al.* 1992; Sage *et al.* 1993; Payseur *et al.* 2004; Teeter *et al.* 2010; Janoušek *et al.* 2012). Although there is evidence for assortative mating between *M. m. musculus* and *M. m. domesticus* (Smadja *et al.* 2004; Smadja and Ganem 2005) and fertility reductions in hybrid females (Good *et al.* 2008b; Suzuki and Nachman 2015), the most consistently documented reproductive barrier is F_1 hybrid male sterility (sterility in this context refers to greatly reduced fertility). Crosses involving wild animals, wild-derived inbred strains, and classical inbred strains produce males with reduced fertility (Forejt and Ivanyi 1974; Chubb and Nolan 1987; Yoshiki *et al.* 1993; Alibert *et al.* 1997; Britton-Davidian *et al.* 2005; Vyskočilová *et al.* 2005; Good *et al.* 2008b; White *et al.* 2011). F_1 hybrid male sterility is polymorphic within *M. m. domesticus* and within *M. m. musculus* (Britton-Davidian *et al.* 2005; Good *et al.* 2008b; Larson *et al.* 2018), an example of the intraspecific variation in intrinsic

Table 1 Testis histology phenotypes and their expected relationships to fertility

Histology phenotype	Process/state measured	Expected pattern in subfertile testis
Testis area	Overall fertility	Lower
Stage VII tubule area	Overall fertility	Lower
Number of Sertoli cells in healthiest stage VII tubule	Support of meiosis	Fewer/same
Number of pachytene spermatocytes in healthiest stage VII tubule	Induction of meiosis	Fewer
Number of round spermatids in healthiest stage VII tubules	Meiotic progression to meiosis II	Fewer
Multinucleated syncytia per testis	Spermatocyte degeneration; failure of spermatogenesis or spermiogenesis	More
Number of tubules with ≥3 apoptotic primary (meiosis I) spermatocytes	Degeneration of developing spermatocytes	More
Number of tubules with ≥3 apoptotic round spermatids	Degeneration of developing spermatids	More

postzygotic isolation observed in a variety of species pairs [reviewed in Cutter (2012)]. In some crosses, a severe reduction in fertility is only found when the mother is *M. m. musculus* (Good *et al.* 2008b).

Much is understood about the genetic basis of F_1 hybrid male sterility between *M. m. domesticus* and *M. m. musculus*. F_1 males from crosses between some strains of *M. m. musculus* and C57BL/10 (a classical inbred strain of predominantly *M. m. domesticus* origin) are effectively sterile, whereas F_1 males from similar crosses using classical strain C3H as the *M. m. domesticus* representative are fertile (Forejt 1996). Forejt and colleagues exploited this polymorphism to identify the first known hybrid sterility gene in vertebrates (Forejt and Ivanyi 1974; Forejt *et al.* 1991; Trachtulec *et al.* 2005; Mihola *et al.* 2009). *Prdm9* is a histone H3 methyltransferase (Hayashi *et al.* 2005) that facilitates double-strand DNA break generation by locally modifying chromatin structure (Baudat *et al.* 2010; Parvanov *et al.* 2010; Paigen and Petkov 2018). In F_1 hybrids between some strains of *M. m. musculus* and *M. m. domesticus*, *Prdm9* alleles contribute to meiotic arrest in primary spermatocytes (Mihola *et al.* 2009). The arrest is caused by incompatibility between the *Prdm9* heterozygous genotype, a *M. m. musculus* allele on the X chromosome (at the *Hstx2* locus), and multiple additional autosomal loci (Dzur-Gejdošova *et al.* 2012). The overall role of the X chromosome in hybrid male sterility is complex, with contributions from multiple segments of the chromosome (Storchová *et al.* 2004; Good *et al.* 2008a), incompatibility with the Y chromosome in addition to the autosomes (Campbell and Nachman 2014), and large numbers of overexpressed genes in sterile F_1 hybrids (Good *et al.* 2010; Bhattacharyya *et al.* 2013; Turner *et al.* 2014; Larson *et al.* 2017). Asynapsis of hetero-subspecific chromosomes modulated by *Prdm9* and *Hstx2* provides a potential mechanism for this hybrid incompatibility (Mihola *et al.* 2009; Bhattacharyya *et al.* 2013, 2014).

Disrupted epistatic interactions between alleles at different loci (such as *Prdm9* and *Hstx2*), known as hybrid incompatibilities, play a major role in hybrid male sterility across a range of species pairs (Coyne and Orr 2004). These incompatibilities are expected to be enriched for recessive alleles (Muller 1942; Masly and Presgraves 2007), which are invisible in F_1 hybrids at autosomal loci. Natural hybrids between *M. m. domesticus* and *M. m. musculus* are highly backcrossed (Teeter *et al.* 2010), suggesting that examination of hybrid male sterility in subsequent generations is crucial for understanding barriers to gene flow in the wild. Genome-wide association mapping in the hybrid zone revealed complex incompatibilities connected to reduced testis weight (Turner and Harr 2014), one of several signs of subfertility in natural hybrids (Turner *et al.* 2012). A suite of quantitative trait loci (QTL) was identified that confer decreased testis weight, reduced sperm count, or abnormal sperm head shape in F_2 hybrids generated by controlled intercrosses (White *et al.* 2011). Detailed histological explanations for decreased testis weight and other phenotypes were not investigated in these studies of sterility in later-generation hybrids.

Multiple mechanisms for functional sterility in hybrid mice are possible, and we hypothesized that histological abnormalities could help define the pathogenesis of decreased fertility. Developmental defects could lead to fewer seminiferous tubules, resulting in smaller testes. Genetic incompatibilities in later-generation hybrids could lead to defective spermatogonial mitosis, meiosis I, meiosis II, or spermiogenesis. It is also possible that hybrid testes lack enough testosterone-secreting interstitial (Leydig) cells to support proper spermatogenesis and spermiogenesis. Hybrid incompatibilities could reduce the number or function of Sertoli cells. Finally, mechanisms leading to hybrid sterility could have minimal histological impact, affecting only spermiogenesis.

In this article, we go beyond the usual examination of endpoint phenotypes in mature sperm to evaluate these potential developmental causes of hybrid male sterility. We use detailed inspection of testis histopathology in a large number of F_2 hybrids between *M. m. domesticus* and *M. m. musculus* to identify and characterize disruptions in key steps of spermatogenesis. We identify problems with completing meiosis I as a major cause of F_2 hybrid male sterility. We

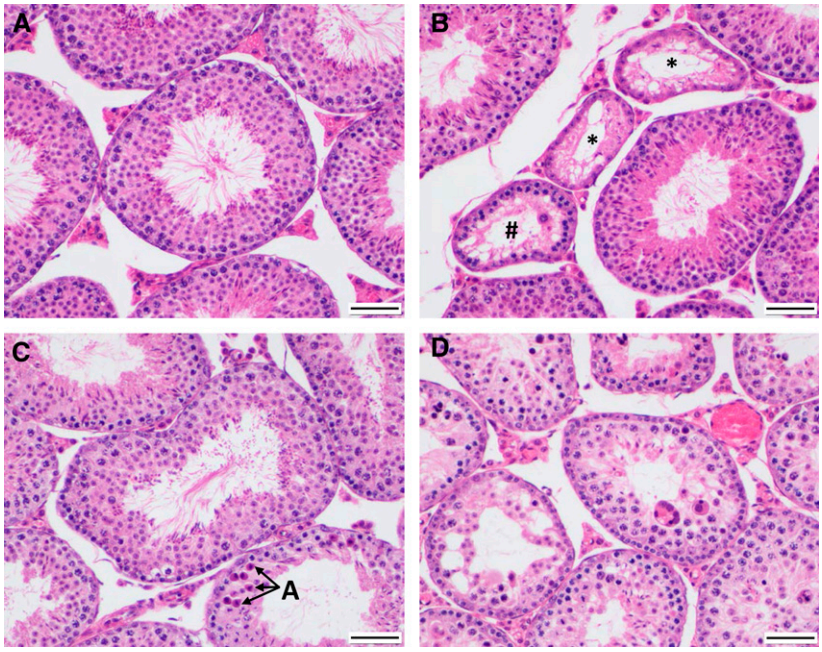

Figure 2 Examples of testis histology phenotypes in parental strains and F_1 hybrids (×200 magnification). (A) Representative *musculus*^{PWD} testis showing multiple tubules containing a plush spermatogenic epithelium. Bar, 50 μm. (B) Representative *domesticus*^{WSB} testis showing several Sertoli-only tubules (indicated by *), commensurate with decreased fertility in this strain. The tubule containing # is atrophic and exhibits a few meiotic cells. Bar, 50 μm. (C) Representative *domesticus*^{WSB} × *musculus*^{PWD} F_1 testis showing mild to moderate degeneration with epithelial thinning and decreased numbers of round spermatids (atrophy) within the spermatogenic epithelium (center tubule) and marked apoptosis (A) of meiosis I cells and round spermatids in an adjacent (lower) tubule. Bar, 50 μm. (D) Representative *musculus*^{PWD} × *domesticus*^{WSB} F_1 testis showing marked degeneration (multinucleated syncytia, apoptosis) and atrophy of the spermatogenic epithelium in multiple tubules. Bar, 50 μm.

proceed to identify QTL for novel indicators of hybrid male sterility, significantly refining the developmental roles of hybrid incompatibilities in the process.

Materials and Methods

Strains and crosses

We used the wild-derived inbred strains WSB/EiJ and PWD/PhJ as representatives of *M. m. domesticus* and *M. m. musculus*, respectively (subsequently denoted as *domesticus*^{WSB} and *musculus*^{PWD}). All testis histology phenotypes reported here were collected from mice generated by White *et al.* (2011) and examined at 70 (±5) days of age. Briefly, *domesticus*^{WSB} and *musculus*^{PWD} were crossed in both directions to produce F_1 hybrids, and F_1 hybrids were sib-mated to generate F_2 hybrids. Testis histology phenotypes were collected from 312 F_2 males. Because F_1 males from *musculus*^{PWD} × *domesticus*^{WSB} crosses (following the convention of listing the mother first) were effectively sterile, 300 of the F_2 males came from the *domesticus*^{WSB} × *musculus*^{PWD} cross direction. Detailed phenotypes were also collected from six *musculus*^{PWD} × *domesticus*^{WSB} F_1 hybrids, six *domesticus*^{WSB} × *musculus*^{PWD} F_1 hybrids, six *musculus*^{PWD}, and six *domesticus*^{WSB}.

Testis histology

Testes were dissected, weighed, fixed overnight in Bouin's fixative, and washed in an ethanol series of 25, 50, and 75%. After standard tissue processing, right testes were bisected across the short axis, embedded in paraffin, sectioned at 5 mm, and stained with hematoxylin and eosin.

Slides were scanned using an Aperio scanner (Leica Biosystems, Buffalo Grove, IL). Digital measurements of testis width and height were taken, and testis area was estimated as an ellipse (Figure 1A). When at least 10 stage VII tubules were present (see below), similar measurements were captured for each of them (Figure 1A) (White *et al.* 2011).

Histology phenotypes

Testes were histologically examined for any phenotypic abnormalities. Once abnormalities were identified, they were scored for distribution and severity. Whenever possible, all testes were scored for a single trait on the same day or on consecutive days. As a threshold screen for further evaluation, we first asked whether each testis had at least 10 stage VII tubules. This approach focused our study on the least-affected testes, thereby decreasing the effects of nonspecific, late-stage testicular degeneration (Figure 1, A and E). Stage VII tubules were chosen for examination because they are readily identifiable, with pachytene spermatocytes and a full lining of elongating spermatids, which are released in stage VIII. Testes with <10 stage VII tubules were not considered further. The number of tubules with at least three apoptotic cells was recorded (Figure 1, B and C). Furthermore, apoptotic cells were identified and recorded as spermatogonia, meiotic cells (Figure 1B), round spermatids (Figure 1C), and/or elongating spermatids. We also recorded the number of multinucleated syncytia in each tubule section, a frequent abnormality in hybrid testes when spermatogonia fail to complete meiosis (Figure 1D). Sertoli cell vacuolation was identified (Figure 1D). Finally, the stage VII tubule in each testis with the thickest spermatogenic epithelium (considered the "healthiest") was identified (Figure 1E) for detailed examination. The rationale for focusing on healthy stage VII tubules was that many of the lesions observed in less healthy tubules were consistent with end-stage disease rather than an active process. By focusing on early changes in the healthiest tubules, we enriched our data set for phenotypes mechanistically connected to hybrid male sterility rather than those common to

Table 2 Testis histology phenotypic means

Phenotype	*domesticus*^{WSB} (n = 6)	*musculus*^{PWD} (n = 6)	*domesticus*^{WSB} × *musculus*^{PWD} F_1 (n = 6)	*musculus*^{PWD} × *domesticus*^{WSB} F_1 (n = 6)	F_2 (n = 312[a])
Testis area (mm^2)	26.7 (5.1)	28.2 (3.1)	30.2 (4.0)	25.6 (5.9)	35.6 (8.1)
Stage VII tubule area[b] ($\mu m^2 \times 10^3$)	44.0 (6.8)[f]	46.3 (2.8)[h,i]	36.4 (1.6)[h,j]	28.2 (1.6)[f,i,j]	42.6 (7.5)
Stage VII Sertoli cells[c]	14.5 (2.9)	11.7 (2.3)	13.5 (2.9)	13.6 (3.2)	15.1 (3.1)
Stage VII pachytene spermatocytes[c]	56.8 (12.3)[f]	57.5 (11.3)[i]	43.7 (9.4)	36.6 (4.7)[f,i]	53.7 (14.8)
Stage VII round spermatids[c]	170.7 (41.3)[f,g]	146.0 (20.8)[h,i]	85.7 (23.0)[g,h,j]	43.80 (24.0)[f,i,j]	137.2 (36.0)
Multinucleated syncytia[d]	2.8 (2.7)[f,g]	0.3 (0.5)[i]	0.0 (0.0)[g,j]	29.5 (8.3)[f,i,j]	3.5 (15.1)
Tubules with apoptosis[g] (meiotic)	0.3 (0.5)	0.0 (0.0)	5.0 (2.6)	N/A	0.5 (1.3)
Tubules with apoptosis[e] (round spermatids)	0.0 (0.0)	0.0 (0.0)	0.2 (0.4)	N/A	0.4 (1.0)

Values reported as mean (SD).
[a] 300 domesticus^{WSB} × musculus^{PWD} cross direction, 12 musculus^{PWD} × domesticus^{WSB} cross direction.
[b] Calculated from the 10 healthiest stage VII tubules in each testis section.
[c] Counts from healthiest tubule in each testis section.
[d] Total count from each testis section.
[e] Scored for tubules with three or more apoptotic cells of respective type.
[f–j] $P < 0.05$ (Mann–Whitney U) in pairwise comparison between groups. F_2s were not included in these comparisons.

degenerative changes in the testis. For each of these stage VII tubules, the number of Sertoli cells, spermatogonia, pachytene spermatocytes, and round spermatids were recorded (Figure 1E). These testis histology phenotypes were also compared to other fertility traits measured in the same mice, including testis weight, tubule area, epididymal sperm count, and epididymal sperm head morphology (White *et al.* 2011). Testis histology phenotypes and their expected relationships to fertility are listed in Table 1.

QTL mapping

Genotypes at 198 informative single nucleotide polymorphisms (SNPs) taken from White *et al.* (2011) were used for QTL mapping. This set of genotypes included SNPs from across the autosomes and the X chromosome. SNPs on the Y chromosome and the mitochondrion were not considered because most F_2 hybrids came from one direction of the intercross. Genotypes were assembled using stringent quality control filters described in Dumont *et al.* (2011) and White *et al.* (2011). Genotypes from a total of 553 F_2 hybrids (males and females) were used to construct a genetic map with the *est.map* procedure and a Carter–Falconer mapping function in R/qtl (Broman *et al.* 2003; White *et al.* 2011). The average distance between SNPs on the genetic map was 7 cM. Physical positions between SNPs were interpolated using genetic and physical positions of flanking SNPs.

We conducted QTL analyses for the following phenotypes: testis area, number of multinucleated syncytia per testis, number of tubules with apoptotic spermatocytes, number of tubules with apoptotic round spermatids, number of tubules containing only Sertoli cells, and the numbers of Sertoli cells, pachytene spermatocytes, and round spermatids (and associated ratios) within the healthiest stage VII tubule. F_2 phenotypic distributions (Supplemental Material, Figure S1) were inspected to determine how each trait should be treated in QTL analyses. The following phenotypes showed non-normal distributions skewed toward the zero-class: tubules with apoptotic meiotic cells, tubules with apoptotic round spermatids, and multinucleated syncytia. These traits were recoded and analyzed as binary presence/absence traits. Numbers of pachytene spermatocytes, round spermatids, and Sertoli cells, as well as testis area, were approximately normally distributed and were analyzed on the observed scale.

QTL were identified using standard interval mapping (Lander and Botstein 1989) or binary interval mapping, implemented using the *scan.one* function in R/qtl. Genome-wide significance thresholds were calculated from 1000 permutations for the autosomes and 15,868 permutations for the X chromosome (Broman *et al.* 2006). Models incorporating multiple QTL were fit using a stepwise forward/backward search algorithm (Manichaikul *et al.* 2009) implemented in the *stepwiseqtl* function in R/qtl, with genome-wide significance thresholds based on 1000 permutations. When multiple QTL were detected for a trait, we performed tests for potential epistatic interactions between detected QTL. Interaction terms for each pair of QTL were added to the multiple-QTL model one at a time, and a P-value for each interaction was calculated based on the improved fit as measured by the F-statistic. All QTL analyses assumed a genotyping error rate of 0.0001. The differential treatment of traits as binary or continuous made it difficult to jointly consider multiple phenotypes in QTL mapping. As a result, we analyzed each trait separately.

Data availability

Phenotypic and genotypic data are available at Data Dryad (http://datadryad.org; DOI: 10.5061/dryad.vd6k4b2). Supplemental material available at Figshare: https://doi.org/10.25386/genetics.7161119.

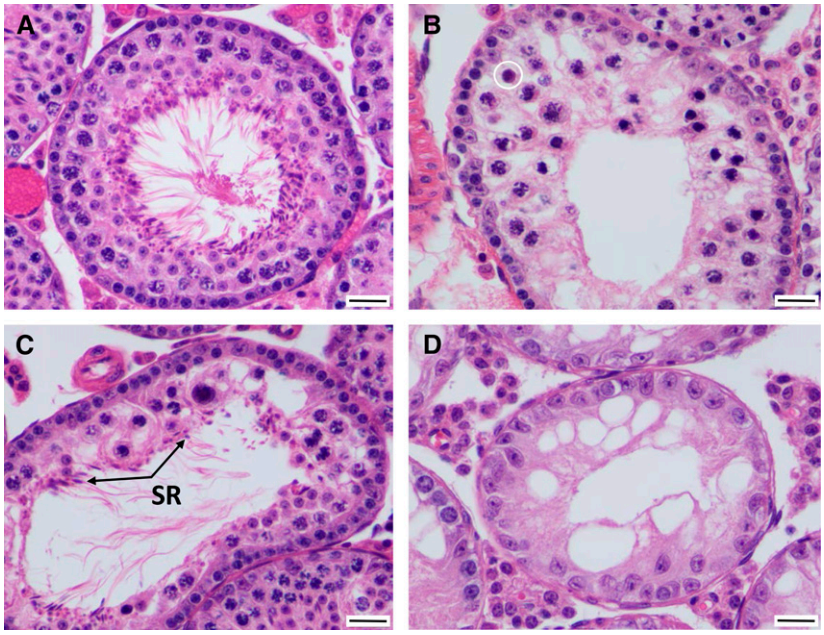

Figure 3 Examples of testis histology phenotypes in stage VII tubules in F_2 hybrids from the *musculus*^{PWD} × *domesticus*^{WSB} cross direction (×400 magnification). (A) In this F_2 tubule, there is a markedly attenuated/atrophic spermatogenic epithelium, consisting of only one or two (rather than three or four) layers of round spermatids. Bar, 20 μm. (B) In this F_2 tubule, there is luminal displacement of primary (meiosis I) spermatocytes, many of which are undergoing apoptosis. There are no maturing round spermatids, and only meiosis I is identified. The circle indicates a meiotic cell entering apoptosis. Bar, 20 μm. (C) In this F_2 tubule, there is marked disruption of spermatogenesis, with only a few meiotic spermatocytes, few round spermatids, formation of a multinucleated syncytium, and spermatid retention (SR), where elongated spermatids are still held by Sertoli cells. Bar, 20 μm. (D) In this (and adjacent) F_2 tubule, there is complete loss of spermatogonia, meiotic spermatocytes, and round spermatids, leaving only Sertoli cells. Bar, 20 μm.

Results

Testis histology in parental strains and F_1 hybrids

musculus^{PWD} testis sections all contain at least 10 stage VII tubules lined by a plush seminiferous epithelium consisting of Sertoli cells, meiotic spermatocytes, at least three layers of secondary spermatocytes and round spermatids (as these two cell types cannot be distinguished histologically, the term "round spermatids" is used throughout to include both), and elongating spermatids (Figure 2A). These animals appeared to be fully fertile in our laboratory (White *et al.* 2011).

domesticus^{WSB} testis sections often contain multiple tubules exhibiting marked atrophy (Figure 2B, #) or complete absence of the spermatogenic epithelium (Figure 2B, *). Tubules that could not be staged because of their degeneration are shrunken and contain heavily or partially vacuolated Sertoli cells (Figure 2B, *) and contain a few meiotic cells (Figure 2B, #), indicating that spermatogonia are still present. These histologic changes likely contribute to this strain's lower fertility (Odet *et al.* 2015), despite its normal sperm density (White *et al.* 2011).

domesticus^{WSB} × *musculus*^{PWD} F_1 testis sections exhibit an intermediate phenotype, with mild atrophy (thinning) of the stage VII spermatogenic epithelium typified by a reduced number of developing round spermatids (generally fewer than three layers; Figure 2C). Apoptosis, as identified by shrunken cells with hyper-eosinophilic cytoplasm and pyknotic nuclei, is increased in these testes (Figure 2C, A in adjacent tubule; Table 2); this may be a mechanism of atrophy in this direction of the cross. *domesticus*^{WSB} × *musculus*^{PWD} F_1 testis sections contain significantly fewer stage VII round spermatids than both parental strains (Table 2). Despite these histopathologic abnormalities, *domesticus*^{WSB} × *musculus*^{PWD} F_1 hybrids bred well in our laboratory (White *et al.* 2011).

Compared to testes from *musculus*^{PWD}, *domesticus*^{WSB}, and *domesticus*^{WSB} × *musculus*^{PWD} F_1 mice, testes from *musculus*^{PWD} × *domesticus*^{WSB} F_1 mice show severe degeneration (Figure 2D and Table 2). The spermatogenic epithelium is highly atrophied, Sertoli cell vacuolation is marked, and multiple multinucleated syncytia are visible (Figure 2D and Table 2). *musculus*^{PWD} × *domesticus*^{WSB} F_1 testes have significantly less stage VII tubule area, fewer stage VII pachytene spermatocytes, and fewer stage VII round spermatids than both parental strains (Table 2). F_1 hybrids from this direction of the cross exhibited very poor fertility in the laboratory setting (White *et al.* 2011).

Testis histology in F_2 hybrids

Testes from *domesticus*^{WSB} × *musculus*^{PWD} F_2 mice present a range of phenotypes that indicate defective spermatogenesis (Figure 3 and Figure S1). The severity of each phenotype is typically milder than seen in either F_1 cross or *domesticus*^{WSB} testes (Table 2). Many *domesticus*^{WSB} × *musculus*^{PWD} F_2 testes show substantial and progressive atrophy of the spermatogenic epithelium, including loss of elongating spermatids (Figure 3, B and C), round spermatids (Figure 3, A–C), meiotic spermatocytes (Figure 3, B and C), and/or spermatogonia (leaving only Sertoli cells; Figure 3D) (Table 2). Normal tubules should contain at least three layers of round spermatids (*e.g.*, Figure 2A), but this is often not the case (*e.g.*, Figure 3A). This result suggests an initial defect in meiosis I. Apoptosis is increased, both within pachytene spermatocytes (again suggesting a defect in meiosis I), and within the more basal layers of round spermatids. Fewer round spermatids are present (Figure S1), suggesting that fewer primary spermatocytes survive to meiosis II and spermiogenesis; this is an expected outcome from an increase in

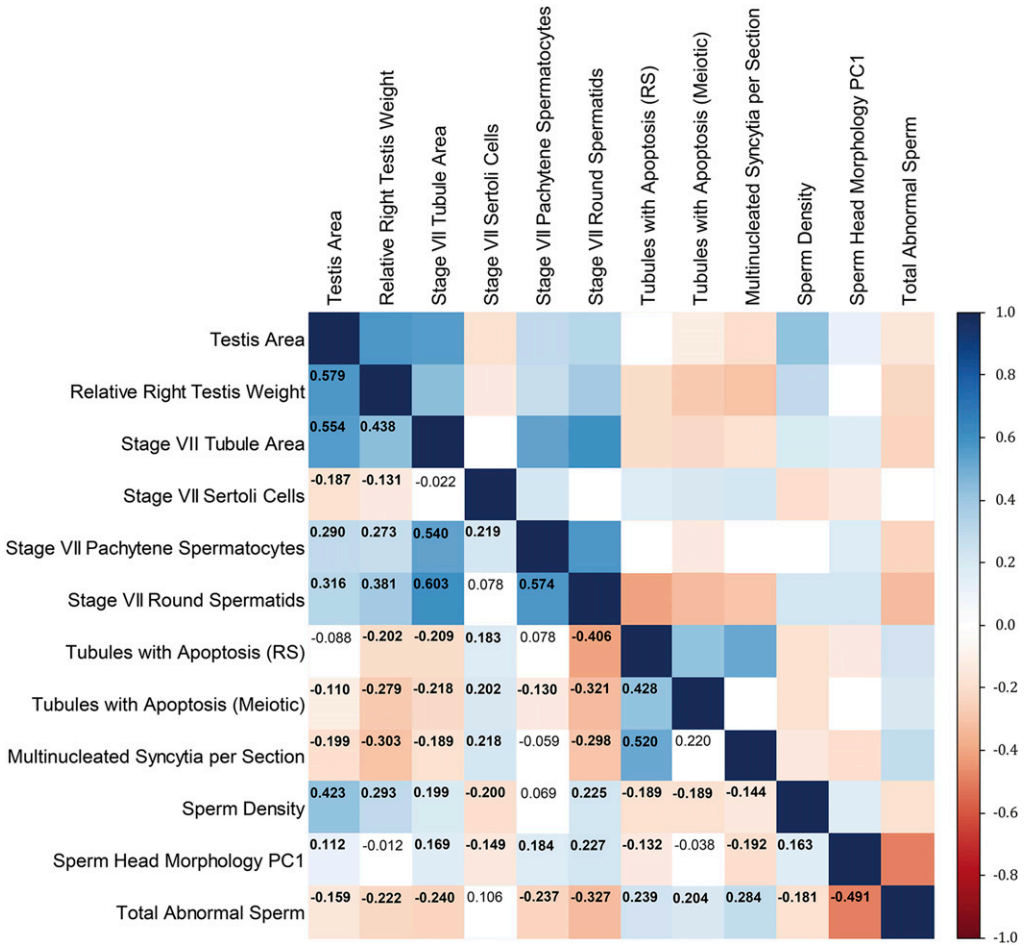

Figure 4 Pearson's correlations among testis histology phenotypes across F_2 mice (displayed as a heat map). Correlations with $P < 0.05$ are bolded. Data for relative right testis weight, stage VII tubule area, sperm density, sperm head morphology PC1, and total abnormal sperm were originally reported in White *et al.* (2011). PC1, principal component 1; RS, round spermatids.

apoptosis within the meiotic I compartment. We observed no increase in apoptosis among spermatogonia.

Some tubules contain abnormal meiotic cells at all levels of the tubule and completely lack round spermatids (Figure 3, B and C). These abnormal cells exhibit densely compacted and clumped chromatin but lack obvious cytoplasmic eosinophilia (Figure 3, B and C). Chromatin clumping is likely associated with early stages of apoptosis, and a few of these abnormal meiotic cells appear to be entering apoptosis (Figure 3B, circle). Pachytene spermatocytes do not accumulate in stage VII tubules, suggesting that meiotic arrest, if it occurs, is brief and apoptosis is rapidly triggered. Additionally, there is no change in the ratio of pachytene spermatocytes to either Sertoli cells or round spermatids that would be indicative of meiotic arrest. The observation that abnormal meiotic cells are found at all levels of the tubule (Figure 3, B and C) when they should be anatomically restricted to the suprabasilar compartment, completing meiosis II and attaining a rounded phenotype, again points to a defect in meiosis I.

Another common sign of degeneration in F_2 testes is the formation of multinucleated syncytial cells from round spermatids, indicating a failure to complete meiosis. Small numbers of multinucleated syncytial cells (0–1 per testis) are expected in healthy testes. The average number of multinucleated syncytia for F_2 testis sections from the *domesticus*^{WSB} × *musculus*^{PWD} cross is 3.5 (SD 15.1) (Table 2). Additionally, a few tubules exhibit a phenomenon known as spermatid retention (Figure 3C). Spermatid retention occurs when elongating spermatids are not released to the lumen of the tubule. It may be caused by the absence of the next wave of developing spermatocytes and loss of their maturation stimuli. Sertoli cell vacuolation is also present, indicating dysfunction of Sertoli cells (Figure 3, B–D). F_2 distributions for testis histology phenotypes used for QTL mapping are shown in Figure S1.

Phenotypic correlations across F_2 hybrids

Our data set provided an unusual opportunity to characterize relationships between different histologic defects associated with hybrid male sterility during the processes of spermatogenesis and spermiogenesis. Across F_2 hybrids, many pairs of traits are significantly correlated (Figure 4). Most correlations are weak in magnitude (Figure 4), suggesting that each trait contains distinct information about hybrid male sterility and motivating the independent treatment of phenotypes in subsequent genetic analyses. A set of stronger correlations highlight temporally and/or functionally connected processes. These relationships include positive correlations between

Table 3 QTL from single QTL analyses

Phenotype	Chromosome	Position (cM)	LOD	Position (Mb)	1.5 LOD interval (Mb)	DD[a]	DM[a]	MM[a]
Testis area (cm^2)	10	18.6	5.76	65.1	40.4–121.1	0.34 (0.01)	0.35 (0.01)	0.40 (0.01)
	X	0.0	2.92	10.2	10.2–166.3	0.38 (0.01)	—	0.34 (0.01)
Multinucleated syncytia[b]	17	13.3	4.26	30.0	3.1–65.2	2.02 (1.80)	5.26 (1.21)	1.14 (1.98)
	X	0.0	8.00	10.2	10.2–58.3	0.95 (1.33)	—	5.78 (1.20)
With tubule area as covariate[c]	8	15.0	4.54	53.6	33.5–66.5	1.51 (1.97)	3.17 (1.25)	6.22 (1.81)
Tubules with apoptosis (round spermatids)[d]	X	0.0	4.81	10.2	10.2–45.1	0.17 (0.09)	—	0.68 (0.08)
Round spermatids per Sertoli cell	17	13.3	4.27	30.0	3.1–65.2	10.1 (0.33)	8.7 (0.22)	10.3 (0.36)
	X	15.0	3.91	58.3	10.2–71.5	10.2 (0.24)	—	8.8 (0.22)
Round spermatids[e] With pachytene as covariate	17	13.3	4.99	30.0	23.3–65.2	140.0 (4.1)	130.5 (2.8)	150.9 (4.5)

D, M. m. domesticus^{WSB}; M, M. m. musculus^{PWD}.
[a] Phenotypic means for each genotype with SE in parenthesis.
[b] Mapped as binary trait, presence of more than one multinucleated syncytium in testis section.
[c] QTL identified when tubule area in testis section is used as a covariate.
[d] Mapped as binary trait, presence or absence of apoptotic cells among round spermatids in testis section.
[e] QTL identified when number of stage VII pachytene spermatocytes are used as a covariate.

numbers of pachytene spermatocytes and round spermatids, numbers of tubules with apoptotic meiotic cells and tubules with apoptotic round spermatids, numbers of tubules with apoptotic round spermatids and multinucleated syncytia, tubule area and number of pachytene spermatocytes, and tubule area and number of round spermatids (Figure 4).

QTL for testis histology defects

Single QTL mapping identified loci linked to five phenotypes (Table 3). Four of these traits are connected to round spermatids: the number of round spermatids (with the number of pachytene spermatocytes as covariate), the number of round spermatids per Sertoli cell, the presence/absence of tubules with apoptotic round spermatids, and the presence/absence of multinucleated syncytia. QTL for testis area also were found.

QTL on chromosome 17 affect the number of round spermatids and the presence of multinucleated syncytia. Heterozygotes for these QTL show phenotypes consistent with reduced fertility, matching the previously reported underdominant effects (on other fertility traits) of this genomic region (Dzur-Gejdošova *et al.* 2012; Flachs *et al.* 2012; Turner *et al.* 2014).

QTL on the X chromosome determine the number of round spermatids per Sertoli cell, the presence of tubules with apoptotic round spermatids, the presence of multinucleated syncytia, and testis area. The estimated position of the QTL for the number of round spermatids per Sertoli cell is 48 Mb distal to the QTL for the other three traits, raising the possibility that the X chromosome contains multiple QTL (although the 1.5 LOD intervals overlap). For each of the four phenotypes, the *musculus*^{PWD} X chromosome is associated with reduced fertility, consistent with previous reports (Storchová *et al.* 2004; White *et al.* 2011).

Some QTL were only identified once variation in other traits was considered. QTL on chromosome 17 for round spermatid number were only detected when this phenotype was divided by the number of Sertoli cells or when the number of pachytene spermatocytes was treated as a covariate. The X-linked QTL only appeared when the number of pachytene spermatocytes was used as a covariate. These conditional mapping results suggest that the relationship between round spermatids and meiotic cells and/or Sertoli cells is an important part of QTL activity on chromosomes 17 and X.

Multiple QTL mapping identified loci linked to the same five phenotypes as single QTL mapping (Table 4). Multiple QTL mapping revealed additional QTL that contribute to the presence of multinucleated syncytia (chromosome 18) and testis area (chromosome 3) (Table 4). For some QTL, 1.5 LOD intervals were narrowed compared to single QTL mapping.

Tests for epistasis revealed a significant interaction between the QTL on chromosomes 17 and X for the presence of multinucleated syncytia (pointwise $P < 0.005$) that explains an additional 3% of the variance. There was no evidence for epistasis between any of the other detected QTL.

We compared QTL positions with those found previously in the same cross for additional traits connected to hybrid male sterility (White *et al.* 2011). The chromosome 17 positions of QTL for the number of round spermatids and the presence of multinucleated syncytia are the same or very similar to QTL for epididymal sperm density. The position of the X-linked QTL for the number of round spermatids is close to QTL for some measures of sperm head morphology. X-linked QTL for the presence of tubules with apoptotic round spermatids and multinucleated syncytia, as well as testis area, are located more proximally than X-linked QTL for sperm head morphology, although there is some overlap in 1.5 LOD intervals. QTL on chromosomes 8 and 18 for the presence of multinucleated syncytia overlap with QTL for seminiferous tubule area. Testis area QTL located on chromosomes 3 and 10 overlap with QTL for relative right testis weight.

Table 4 QTL from multiple QTL analyses

Phenotype	Chromosome	Position (cM)	LOD	Position (Mb)	1.5 LOD interval (Mb)	% Variance[a]	Additive effect[b]	Dominance deviation[c]
Testis area (cm^2)	3	52.0	3.62	125.0	97.2–141.0	4.9	−0.62 (0.2)	−0.88 (0.3)
	10	19.0	5.35	66.4	49.5–82.7	7.3	0.87 (0.2)	−0.80 (0.3)
	X	0.0	3.47	10.2	10.2–56.4	4.7	−0.57 (0.1)	—
Multinucleated syncytia[d]	17	12.0	4.46	26.9	8.9–44.0	5.7	−0.52 (3.5)	22 (4.8)
	18	36.0	3.80	71.9	61.5–82.8	4.8	4.8 (3.5)	20 (4.9)
	X	1.0	8.03	14.4	10.2–54.4	10.5	15 (2.4)	—
Multinucleated syncytia[d]	8	15.0	3.84	53.6	35.5–66.5	5.4	14 (3.4)	1.8 (4.9)
With tubule area as covariate	17	13.0	4.18	29.2	10.8–44.0	5.9	−0.91 (3.3)	20 (4.6)
	X	0.0	4.83	10.2	10.2–91.9	6.9	11 (2.3)	—
Tubules with apoptosis (round spermatids)[e]	X	0.0	4.67	10.2	10.2–44.2	7.2	12 (2.5)	—
Round spermatids per Sertoli cell	17	12.0	4.20	26.9	6.9–60.1	6.1	−4.4 (24)	−147 (33)
	X	11.0	4.00	50.5	10.2–70.1	5.8	−73 (17)	—
Round spermatids[f] With pachytene as covariate	17	13.3	4.98	29.9	6.9–53.4	5.0	512 (244)	−1487 (330)

Values in effect columns scaled by 10^2.

[a] Percentage of phenotypic variance explained by QTL.

[b] Additive effects calculated as half the difference between phenotypic average of homozygotes, estimated effect with SE in parentheses.

[c] Dominance deviation calculated as difference between phenotypic average of heterozygotes and the midpoint between phenotypic averages of homozygotes, estimated deviation with SE in parenthesis.

[d] Mapped as binary trait, presence of more than one multinucleated syncytium in testis section. Using tubule area as a covariate produces a best-fitting model with a differing set of QTL.

[e] Mapped as binary trait, presence or absence of apoptotic cells among round spermatids in testis section.

[f] QTL identified when number of stage VII pachytene spermatocytes is used as a covariate.

A schematic summarizing QTL activities in the temporal context of spermatogenesis and spermiogenesis is provided in Figure 5.

Discussion

The continuous and spatially structured nature of spermatogenesis makes it possible to assign abnormalities to specific stages and processes through detailed histological examination of testes. Our application of this strategy to a large sample of hybrid mouse testes elucidated the phenotypic and genetic causes of a primary reproductive barrier—hybrid male sterility—between two subspecies of house mice.

Phenotypic determinants of F_2 hybrid male sterility

Although we found significant phenotypic heterogeneity across F_2 mice, a few overall patterns point to the developmental bases of F_2 hybrid male sterility. Testes generally develop normally, as indicated by the presence of interstitial (Leydig) cells, Sertoli cells, seminiferous tubules, and spermatogonia in expected numbers. Active division and entry into meiosis of spermatogonia show that mitosis proceeds normally.

Increases in apoptotic pachytene meiotic cells and decreases in round spermatids suggest that the failure to complete meiosis I is a primary barrier. This failure leads to increased apoptosis within round spermatids and an increase in multinucleated syncytia (degenerating spermatids). Our results are consistent with cell death by activation of the pachytene checkpoint in meiosis I in hybrids. As secondary spermatocytes and round spermatids cannot be histologically distinguished, and an increase in apoptotic round spermatids was noted, the possibility exists of an additional downstream defect in meiosis II. Identification of multinucleated syncytia also suggests potential postmeiotic defects in spermiogenesis, although syncytia can result from aberrant meiosis as well.

Although F_2 hybrids harbor normal numbers of Sertoli cells, Sertoli cell vacuolation in some tubules suggests dysfunction of these cells as well. The frequency of tubules with vacuolation is associated with infertility in extinct lines from the Collaborative Cross (Shorter *et al.* 2017), which are themselves hybrids of three subspecies of house mice (Threadgill and Churchill 2012). Sertoli cells form the blood–testis barrier, which prevents the immune system from attacking the genetically novel cells generated by meiosis. We attribute Sertoli cell vacuolation to a loss of trophic feedback from developing spermatocytes held within the Sertoli cells; these two cell types are cytoplasmically linked via gap junctions.

Our study is the first to comprehensively characterize testis histology in hundreds of hybrid mice. Comparisons to other studies of hybrids that reported testis histology in smaller numbers of mice reveal potential generalities. Wild hybrids from the European contact zone between *M. m. domesticus* and *M. m. musculus* exhibit some of the same testicular abnormalities we identified, including significant apoptosis of round spermatids, vacuolated Sertoli cells, multinucleated

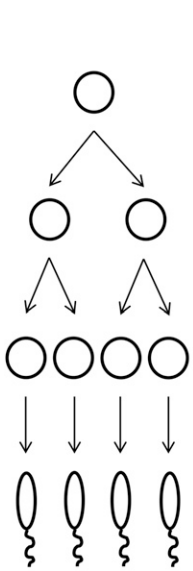

Figure 5 Schematic illustrating phenotypic effects of F_2 hybrid male sterility QTL.

syncytia, and spermatid retention (Turner *et al.* 2012). The apoptosis we detected in laboratory-reared F_2 hybrids was earlier (in pachytene spermatocytes) than that observed in natural hybrids (chiefly round spermatids) (Turner *et al.* 2012). Nevertheless, the overall histologic similarities suggest that F_2 hybrid mice generated in the laboratory provide strong models for reductions in hybrid fertility in the wild.

The defects we observed in F_1 hybrids were less severe than those previously reported for sterile F_1 hybrids from crosses between two *M. m. musculus* strains and C57BL/6 (an inbred strain mostly descended from *M. m. domesticus*). Testes from NJL × C57BL/6 F_1 hybrids contain spermatogonia and primary spermatocytes, but no secondary spermatocytes or spermatids (Kaku *et al.* 1995). Testes from these hybrids undergo primary spermatocyte apoptosis and harbor a reduced number of pachytene cells relative to zygotene cells (Oka *et al.* 2010). Testes from *musculus*^{PWD} × C57BL/6 F_1 hybrids completely lack postmeiotic cells, with apoptosis in meiosis I leading to a deficiency in the number of midpachytene cells and an absence of diplotene cells (Bhattacharyya *et al.* 2013). Testes from *musculus*^{PWD} × *domesticus*^{WSB} F_1 hybrids show similarly drastic signs of reduced fertility. Like other traits associated with hybrid male sterility (Good *et al.* 2008b), testis histology in F_1 hybrids between *M. m. musculus* and *M. m. domesticus* differs among strains. Another factor that complicates comparisons among studies is that tubule degeneration results in Sertoli-only tubules lacking primary and secondary spermatocytes. As a result, studies of older mice could miss the primary degenerative process, instead revealing the end-stage (infertile) testis consisting of chiefly Sertoli-only tubules.

Genetic determinants of F_2 hybrid male sterility

We used substantial variation in testis histology phenotypes among F_2 mice to identify QTL that contribute to a subset of these traits. Our study is the first to characterize the genetic architecture of these five measures of testis abnormalities.

Our results indicate important roles for loci on multiple chromosomes in the development of F_2 hybrid male sterility. The effects of QTL on chromosomes 17 and X on testis histology mirror those previously documented for other sterility traits in F_1 hybrids and in consomics/congenics (Forejt and Ivanyi 1974; Forejt *et al.* 1991; Storchová *et al.* 2004; Mihola *et al.* 2009; Dzur-Gejdošova *et al.* 2012). In particular, mice heterozygous for chromosome 17 QTL and/or carrying chromosome X QTL alleles from *musculus*^{PWD} show histologic traits associated with reduced fertility.

The underdominant action and genomic positions of the QTL on chromosome 17 suggest the causative mutation(s) lie(s) in *Prdm9* (Mihola *et al.* 2009). If this turns out to be the case, our results would extend the phenotypic effects of *Prdm9*-based incompatibilities to include multinucleated syncytia. Our findings would also confirm that these incompatibilities reduce the number of round spermatids in F_2 hybrids. Furthermore, these patterns are consistent with the hypothesis that *Prdm9*-based incompatibilities cause F_1 hybrid male sterility by triggering pachytene checkpoint activation in meiotic prophase I with reductions in synapsis and double-strand-break repair (Bhattacharyya *et al.* 2013; Gregorova *et al.* 2018). The estimated positions of QTL on chromosome 17 reported here and in White *et al.* (2011) (~26–30 Mb) are far enough away from the location of *Prdm9* (15.5 Mb) to raise the possibility that this gene is not the causative locus (although the confidence intervals include *Prdm9*). Reaching a definitive conclusion will require finer genetic mapping in this genomic region.

Testis area, the presence of tubules with apoptotic round spermatids, and the presence of multinucleated syncytia all map to the proximal part of the X chromosome. These results suggest that this X-linked region primarily affects apoptosis,

leading to both decreased testis area (due to loss of spermatocytes) and subsequent formation of multinucleated syncytia (degenerate spermatocytes). Based on position, QTL in this region appear to be distinct from previously reported F_1 hybrid male sterility QTL *Hst1x* (which disrupts spermiogenesis) (Storchová *et al.* 2004) and *Hst2x* (which arrests meiosis) (Bhattacharyya *et al.* 2014). Introgression of the proximal third of the X chromosome from the PWK strain of *M. m. musculus* on to the genomic background of the LEWES strain of *M. m. domesticus* also reduces sperm count and testis weight (Good *et al.* 2008a). Our results suggest that a second QTL on the X chromosome controls the number of round spermatids (although confidence intervals on position overlap). Overall, our findings support the idea that the X chromosome contributes to hybrid male sterility in multiple ways (Storchová *et al.* 2004; Good *et al.* 2008a, 2010; Bhattacharyya *et al.* 2014; Turner *et al.* 2014; Larson *et al.* 2017).

QTL for multinucleated syncytia on chromosomes 8 and 18 localize near QTL for seminiferous tubule area (White *et al.* 2011). Syncytia indicate failures in differentiation from round spermatids to spermatozoa, as the preexisting junctions between these cells fail to separate and the cells are not released from Sertoli cells. Because multinucleated syncytial cells represent spermatocyte degeneration, spermatocyte loss is also likely; this in turn could reduce tubule area. The overlap of QTL for testis area with QTL for testis weight (White *et al.* 2011) suggests that these loci control the overall size of the testis in hybrids.

The absence of QTL for other histologic traits could indicate that these phenotypes are not important contributors to hybrid male sterility in this cross. In this vein, most F_2 hybrids could be characterized as displaying normal aspects of testis development (as revealed by the numbers of tubules and Sertoli cells) and normal initiation of meiosis I (as revealed by the number of pachytene spermatocytes). Alternatively, genetic incompatibilities could exist for these traits, but with effects too small to detect using our sample size. Finally, these phenotypes could feature higher measurement error, although we have no indication that this is the case.

Examination of testis abnormalities in intercrosses featuring other strains could identify different QTL or distinct phenotypic effects of the same QTL. Both *M. m. domesticus* and *M. m. musculus* subspecies harbor polymorphism for F_1 hybrid male sterility involving chromosomes X (Good *et al.* 2008b) and 17 (Forejt and Ivanyi 1974; Vyskočilová *et al.* 2009), and other autosomes (Larson *et al.* 2018). Detailed examination of testis histology in crosses with other subspecies of house mice, including *M. m. castaneus*, would help resolve the evolutionary origins of the hybrid incompatibilities we identified (Moyle and Payseur 2009; White *et al.* 2012; Wang *et al.* 2015).

Acknowledgments

We gratefully acknowledge the expert technical assistance of Beth Gray with slide preparation. We thank Daniel Barbash and two anonymous reviewers for helpful feedback on the manuscript. R.J.W. and M.A.W. were both supported by a National Institutes of Health (NIH) training grant in Genetics (T32 GM007133) and an NIH training grant in Computation and Informatics in Biology and Medicine (T15 NLM2M007359). R.J.W. was also supported by a University of Wisconsin-Madison Science and Medicine Graduate Research Scholarship. This research was supported by National Science Foundation grants DEB1353737 and DEB0918000, and NIH grant R01 GM120051 to B.A.P.

Literature Cited

Alibert, P., F. Fel-Clair, K. Manolakou, J. Britton-Davidian, and J. C. Auffray, 1997 Developmental stability, fitness, and trait size in laboratory hybrids between European subspecies of the house mouse. Evolution 51: 1284–1295. https://doi.org/10.1111/j.1558-5646.1997.tb03975.x

Baudat, F., J. Buard, C. Grey, A. Fledel-Alon, C. Ober *et al.*, 2010 PRDM9 is a major determinant of meiotic recombination hotspots in humans and mice. Science 327: 836–840. https://doi.org/10.1126/science.1183439

Bhattacharyya, T., S. Gregorova, O. Mihola, M. Anger, J. Sebestova *et al.*, 2013 Mechanistic basis of infertility of mouse intersubspecific hybrids. Proc. Natl. Acad. Sci. USA 110: E468–E477. https://doi.org/10.1073/pnas.1219126110

Bhattacharyya, T., R. Reifova, S. Gregorova, P. Simecek, V. Gergelits *et al.*, 2014 X chromosome control of meiotic chromosome synapsis in mouse inter-subspecific hybrids. PLoS Genet. 10: e1004088. https://doi.org/10.1371/journal.pgen.1004088

Boursot, P., J. C. Auffray, J. Britton-Davidian, and F. Bonhomme, 1993 The evolution of house mice. Annu. Rev. Ecol. Syst. 24: 119–152. https://doi.org/10.1146/annurev.es.24.110193.001003

Britton-Davidian, J., F. Fel-Clair, J. Lopez, P. Alibert, and P. Boursot, 2005 Postzygotic isolation between the two European subspecies of the house mouse: estimates from fertility patterns in wild and laboratory-bred hybrids. Biol. J. Linn. Soc. Lond. 84: 379–393. https://doi.org/10.1111/j.1095-8312.2005.00441.x

Broman, K. W., H. Wu, S. Sen, and G. A. Churchill, 2003 R/qtl: QTL mapping in experimental crosses. Bioinformatics 19: 889–890. https://doi.org/10.1093/bioinformatics/btg112

Broman, K. W., S. Sen, S. E. Owens, A. Manichaikul, E. M. Southard-Smith *et al.*, 2006 The X chromosome in quantitative trait locus mapping. Genetics 174: 2151–2158. https://doi.org/10.1534/genetics.106.061176

Campbell, P., and M. W. Nachman, 2014 X-Y interactions underlie sperm head abnormality in hybrid male house mice. Genetics 196: 1231–1240. https://doi.org/10.1534/genetics.114.161703

Chubb, C., and C. Nolan, 1987 Mouse hybrid sterility and testicular function. Biol. Reprod. 36: 1343–1348. https://doi.org/10.1095/biolreprod36.5.1343

Coyne, J. A., and H. A. Orr, 1989 Patterns of speciation in Drosophila. Evolution 43: 362–381. https://doi.org/10.1111/j.1558-5646.1989.tb04233.x

Coyne, J. A., and H. A. Orr, 2004 *Speciation*. Sinauer Associates, Sunderland, MA.

Cutter, A. D., 2012 The polymorphic prelude to Bateson-Dobzhansky-Muller incompatibilities. Trends Ecol. Evol. 27: 209–218. https://doi.org/10.1016/j.tree.2011.11.004

Dumont, B. L., M. A. White, B. Steffy, T. Wiltshire, and B. A. Payseur, 2011 Extensive recombination rate variation in the house mouse species complex inferred from genetic linkage maps. Genome Res. 21: 114–125. https://doi.org/10.1101/gr.111252.110

Duvaux, L., K. Belkhir, M. Boulesteix, and P. Boursot, 2011 Isolation and gene flow: inferring the speciation history of European house mice. Mol. Ecol. 20: 5248–5264. https://doi.org/10.1111/j.1365-294X.2011.05343.x

Dzur-Gejdošova, M., P. Simecek, S. Gregorova, T. Bhattacharyya, and J. Forejt, 2012 Dissecting the genetic architecture of F1 hybrid sterility in house mice. Evolution. 66: 3321–3335. https://doi.org/10.1111/j.1558-5646.2012.01684.x

Flachs, P., O. Mihola, P. Šimeček, S. Gregorová, J. C. Schimenti *et al*., 2012 Interallelic and intergenic incompatibilities of the Prdm9 (Hst1) gene in mouse hybrid sterility. PLoS Genet. 8: e1003044. https://doi.org/10.1371/journal.pgen.1003044

Forejt, J., 1996 Hybrid sterility in the mouse. Trends Genet. 12: 412–417. https://doi.org/10.1016/0168-9525(96)10040-8

Forejt, J., and P. Ivanyi, 1974 Genetic studies on male sterility of hybrids between laboratory and wild mice (Mus musculus L.). Genet. Res. 24: 189–206. https://doi.org/10.1017/S0016672300015214

Forejt, J., V. Vincek, J. Klein, H. Lehrach, and M. Loudovamickova, 1991 Genetic mapping of the T-complex region on mouse chromosome 17 including the hybrid sterility-1 gene. Mamm. Genome 1: 84–91. https://doi.org/10.1007/BF02443783

Geraldes, A., P. Basset, K. L. Smith, and M. W. Nachman, 2011 Higher differentiation among subspecies of the house mouse (Mus musculus) in genomic regions with low recombination. Mol. Ecol. 20: 4722–4736. https://doi.org/10.1111/j.1365-294X.2011.05285.x

Good, J. M., M. D. Dean, and M. W. Nachman, 2008a A complex genetic basis to X-linked hybrid male sterility between two species of house mice. Genetics 179: 2213–2228. https://doi.org/10.1534/genetics.107.085340

Good, J. M., M. A. Handel, and M. W. Nachman, 2008b Asymmetry and polymorphism of hybrid male sterility during the early stages of speciation in house mice. Evolution. 62: 50–65.

Good, J. M., T. Giger, M. D. Dean, and M. W. Nachman, 2010 Widespread over-expression of the X chromosome in sterile F1 hybrid mice. PLoS Genet. 6: e1001148. https://doi.org/10.1371/journal.pgen.1001148

Gregorova, S., V. Gergelits, I. Chvatalova, T. Bhattacharyya, B. Valiskova *et al*., 2018 Modulation of *Prdm9*-controlled meiotic chromosome asynapsis overrides hybrid sterility in mice. eLife 7: e34282. https://doi.org/10.7554/eLife.34282

Hayashi, K., K. Yoshida, and Y. Matsui, 2005 A histone H3 methyltransferase controls epigenetic events required for meiotic prophase. Nature 438: 374–378. https://doi.org/10.1038/nature04112

Janoušek, V., L. Wang, K. Luzynski, P. Dufkova, M. M. Vyskocilova *et al*., 2012 Genome-wide architecture of reproductive isolation in a naturally occurring hybrid zone between Mus musculus musculus and M. m. domesticus. Mol. Ecol. 21: 3032–3047. https://doi.org/10.1111/j.1365-294X.2012.05583.x

Kaku, Y., Y. Kon, N. Takagi, T. Yamashita, M. Hayashi *et al*., 1995 Histological analysis of male hybrid sterility induced by the Hst-1 gene in mice. J. Vet. Med. Sci. 57: 973–975. https://doi.org/10.1292/jvms.57.973

Lander, E. S., and D. Botstein, 1989 Mapping Mendelian factors underlying quantitative traits using RFLP linkage maps. Genetics 121: 185–199.

Larson, E. L., S. Keeble, D. Vanderpool, M. D. Dean, and J. M. Good, 2017 The composite regulatory basis of the large X-effect in mouse speciation. Mol. Biol. Evol. 34: 282–295. https://doi.org/10.1093/molbev/msw243

Larson, E. L., D. Vanderpool, B. A. J. Sarver, C. Callahan, S. Keeble *et al*., 2018 The evolution of polymorphic hybrid incompatibilities in house mice. Genetics 209: 845–859.

Manichaikul, A., J. Y. Moon, S. Sen, B. S. Yandell, and K. W. Broman, 2009 A model selection approach for the identification of quantitative trait loci in experimental crosses, allowing epistasis. Genetics 181: 1077–1086. https://doi.org/10.1534/genetics.108.094565

Masly, J. P., and D. C. Presgraves, 2007 High-resolution genome-wide dissection of the two rules of speciation in Drosophila. PLoS Biol. 5: e243. https://doi.org/10.1371/journal.pbio.0050243

Mihola, O., Z. Trachtulec, C. Vlcek, J. C. Schimenti, and J. Forejt, 2009 A mouse speciation gene encodes a meiotic histone H3 methyltransferase. Science 323: 373–375. https://doi.org/10.1126/science.1163601

Moyle, L. C., and B. A. Payseur, 2009 Reproductive isolation grows on trees. Trends Ecol. Evol. 24: 591–598. https://doi.org/10.1016/j.tree.2009.05.010

Muller, H. J., 1942 Isolating mechanisms, evolution, and temperature. Biol. Symp. 6: 71–125.

Odet, F., W. Pan, T. A. Bell, S. G. Goodson, A. M. Stevans *et al*., 2015 The founder strains of the collaborative cross express a complex combination of advantageous and deleterious traits for male reproduction. G3 (Bethesda) 5: 2671–2683. https://doi.org/10.1534/g3.115.020172

Oka, A., A. Mita, Y. Takada, H. Koseki, and T. Shiroishi, 2010 Reproductive isolation in hybrid mice due to spermatogenesis defects at three meiotic stages. Genetics 186: 339–351. https://doi.org/10.1534/genetics.110.118976

Paigen, K., and P. M. Petkov, 2018 PRDM9 and its role in genetic recombination. Trends Genet. 34: 291–300. https://doi.org/10.1016/j.tig.2017.12.017

Parvanov, E. D., P. M. Petkov, and K. Paigen, 2010 Prdm9 controls activation of mammalian recombination hotspots. Science 327: 835. https://doi.org/10.1126/science.1181495

Payseur, B. A., J. G. Krenz, and M. W. Nachman, 2004 Differential patterns of introgression across the X chromosome in a hybrid zone between two species of house mice. Evolution 58: 2064–2078. https://doi.org/10.1111/j.0014-3820.2004.tb00490.x

Sage, R. D., W. R. Atchley, and E. Capanna, 1993 House mice as models in systematic biology. Syst. Biol. 42: 523–561. https://doi.org/10.1093/sysbio/42.4.523

Shorter, J. R., F. Odet, D. L. Aylor, W. Pan, C. Y. Kao *et al*., 2017 Male infertility is responsible for nearly half of the extinction observed in the mouse collaborative cross. Genetics 206: 557–572. https://doi.org/10.1534/genetics.116.199596

Smadja, C., and G. Ganem, 2005 Asymmetrical reproductive character displacement in the house mouse. J. Evol. Biol. 18: 1485–1493. https://doi.org/10.1111/j.1420-9101.2005.00944.x

Smadja, G., J. Catalan, and C. Ganem, 2004 Strong premating divergence in a unimodal hybrid zone between two subspecies of the house mouse. J. Evol. Biol. 17: 165–176. https://doi.org/10.1046/j.1420-9101.2003.00647.x

Storchová, R., S. Gregorová, D. Buckiová, V. Kyselová, P. Divina *et al*., 2004 Genetic analysis of X-linked hybrid sterility in the house mouse. Mamm. Genome 15: 515–524. https://doi.org/10.1007/s00335-004-2386-0

Suzuki, T. A., and M. W. Nachman, 2015 Speciation and reduced hybrid female fertility in house mice. Evolution. 69: 2468–2481. https://doi.org/10.1111/evo.12747

Teeter, K. C., L. M. Thibodeau, Z. Gompert, C. A. Buerkle, M. W. Nachman *et al*., 2010 The variable genomic architecture of isolation between hybridizing species of house mice. Evolution. 64: 472–485. https://doi.org/10.1111/j.1558-5646.2009.00846.x

Threadgill, D. W., and G. A. Churchill, 2012 Ten years of the collaborative cross. Genetics 190: 291–294. https://doi.org/10.1534/genetics.111.138032

Trachtulec, Z., O. Mihola, C. Vlcek, H. Himmelbauer, V. Paces *et al*., 2005 Positional cloning of the Hybrid sterility 1 gene: fine genetic mapping and evaluation of two candidate genes. Biol.

J. Linn. Soc. Lond. 84: 637–641. https://doi.org/10.1111/j.1095-8312.2005.00460.x

Tucker, P. K., R. D. Sage, J. Warner, A. C. Wilson, and E. M. Eicher, 1992 Abrupt cline for sex chromosomes in a hybrid zone between two species of mice. Evolution 46: 1146–1163. https://doi.org/10.1111/j.1558-5646.1992.tb00625.x

Turner, L. M., and B. Harr, 2014 Genome-wide mapping in a house mouse hybrid zone reveals hybrid sterility loci and Dobzhansky-Muller interactions. eLife 3: e02504. https://doi.org/10.7554/eLife.02504

Turner, L. M., D. J. Schwahn, and B. Harr, 2012 Reduced male fertility is common but highly variable in form and severity in a natural house mouse hybrid zone. Evolution. 66: 443–458. https://doi.org/10.1111/j.1558-5646.2011.01445.x

Turner, L. M., M. A. White, D. Tautz, and B. A. Payseur, 2014 Genomic networks of hybrid sterility. PLoS Genet. 10: e1004162. https://doi.org/10.1371/journal.pgen.1004162

Vyskočilová, M., Z. Trachtulec, J. Forejt, and J. Pialek, 2005 Does geography matter in hybrid sterility in house mice? Biol. J. Linn. Soc. Lond. 84: 663–674. https://doi.org/10.1111/j.1095-8312.2005.00463.x

Vyskočilová, M., G. Pražanová, and J. Piálek, 2009 Polymorphism in hybrid male sterility in wild-derived Mus musculus musculus strains on proximal chromosome 17. Mamm. Genome 20: 83–91. https://doi.org/10.1007/s00335-008-9164-3

Wang, R. J., M. A. White, and B. A. Payseur, 2015 The pace of hybrid incompatibility evolution in house mice. Genetics 201: 229–242. https://doi.org/10.1534/genetics.115.179499

White, M. A., B. Steffy, T. Wiltshire, and B. A. Payseur, 2011 Genetic dissection of a key reproductive barrier between nascent species of house mice. Genetics 189: 289–304. https://doi.org/10.1534/genetics.111.129171

White, M. A., M. Stubbings, B. L. Dumont, and B. A. Payseur, 2012 Genetics and evolution of hybrid male sterility in house mice. Genetics 191: 917–934. https://doi.org/10.1534/genetics.112.140251

Yoshiki, A., K. Moriwaki, T. Sakakura, and M. Kusakabe, 1993 Histological studies on male sterility of hybrids between laboratory and wild mouse strains. Dev. Growth Differ. 35: 271–281. https://doi.org/10.1111/j.1440-169X.1993.00271.x

Communicating editor: D. Barbash